Can Non-Mechanical Proteins Withstand Force? Stretching Barnase by Atomic Force Microscopy and Molecular Dynamics Simulation

Robert B. Best,* Bin Li,† Annette Steward,* Valerie Daggett,† and Jane Clarke*
*Department of Chemistry, University of Cambridge, MRC Centre for Protein Engineering, Cambridge CB2 1EW, United Kingdom; and †Department of Medicinal Chemistry, University of Washington, Seattle, Washington 98195-7610 USA

ABSTRACT Atomic force microscopy (AFM) experiments have provided intriguing insights into the mechanical unfolding of proteins such as titin I27 from muscle, but will the same be possible for proteins that are not physiologically required to resist force? We report the results of AFM experiments on the forced unfolding of barnase in a chimeric construct with I27. Both modules are independently folded and stable in this construct and have the same thermodynamic and kinetic properties as the isolated proteins. I27 can be identified in the AFM traces based on its previous characterization, and distinct, irregular low-force peaks are observed for barnase. Molecular dynamics simulations of barnase unfolding also show that it unfolds at lower forces than proteins with mechanical function. The unfolding pathway involves the unraveling of the protein from the termini, with much more native-like secondary and tertiary structure being retained in the transition state than is observed in simulations of thermal unfolding or experimentally, using chemical denaturant. Our results suggest that proteins that are not selected for tensile strength may not resist force in the same way as those that are, and that proteins with similar unfolding rates in solution need not have comparable unfolding properties under force.

INTRODUCTION

Understanding the pathway by which proteins fold is an established problem that has been investigated using a wide range of biophysical and theoretical techniques. Recently, atomic force microscopy (AFM) has been used in force mode to observe the unfolding of individual immunoglobulin modules in the giant muscle protein titin as it is stretched (Rief et al., 1997). The technique has been extended to the study of other proteins that naturally occur as tandem repeats of similar modules, such as the all-α protein spectrin (Rief et al., 1999) and all-β fibronectin type III domains from titin and human tenascin (Oberhauser et al., 1998; Rief et al., 1998b) (for recent reviews of this application of AFM, see Clausen-Schaumann et al., 2000; Fisher et al., 2000; Janshoff et al., 2000). AFM offers an alternative to traditional solution experiments on protein folding that use chemical denaturants such as guanidine hydrochloride to unfold the protein, and it allows the unfolding properties determined by chemical denaturation to be compared with those under force (Carrion-Vazquez et al., 1999). Single-molecule studies such as these have the additional advantage of being directly comparable to single-molecule pulling simulations (Klimov and Thirumalai, 2000; Zhang et al., 1999), particularly atomistic molecular dynamics (MD) simulations (Izrailev et al., 1999; B. Li, D. O. V. Alonso, B. J. Bennion, and V. Daggett, submitted for publication; Lu et al., 1998; Lu and Schulten, 2000; Paci and Karplus, 1999, 2000). The comparison is further facilitated by having a well-defined molecular reaction coordinate, namely end-to-end distance or extension length, built into the experiment; the analogous quantity in chemical denaturation studies is more nebulous. Indeed, a single property is a poor reaction coordinate for protein unfolding by denaturant or high temperature (Alonso et al., 2001).

Most AFM studies on protein folding thus far have concentrated on proteins that occur naturally as tandem repeats of similar modules: tenascin, spectrin, and titin. All of these domains require tensile strength for their physiological function and may be expected to withstand force. Here, we seek to establish whether proteins that are not normally stretched will be similarly resistant to force and whether AFM will be useful as a technique for the study of any protein of interest. We have chosen to focus on the small globular RNase barnase, which has been extensively studied as a paradigm for folding using both experimental and simulation techniques (Li and Daggett, 1998; Matouschek et al., 1992; Serrano et al., 1992). In barnase, the main hydrophobic core is formed by the packing of the N-terminal α_1 helix against one side of a five-stranded β-sheet (Fig. 1 *a*), and there are two smaller hydrophobic cores, one formed through the packing of the short α_2 and α_3 helices and first strand of the β-sheet, and the other by two short loop regions and the other side of the β-sheet. For comparison, the structure of a titin I27 (TI I27) module that is used as an internal reference is shown in Fig. 1 *b*.

To unambiguously analyze the force traces obtained from AFM force mode experiments, it is desirable to pull a protein comprising a single type of domain arranged in tandem, rather than naturally occurring arrays of different domains (Carrion-Vazquez et al., 1999). The protein folding model T4 lysozyme was polymerized in the solid state by

Received for publication 29 March 2001 and in final form 27 June 2001.
Address reprint requests to Dr. Jane Clarke, Department of Chemistry, University of Cambridge, Lensfield Road, Cambridge CB2 1EW, United Kingdom. Tel.: 44-1223-336426; Fax: 44-1223-336362; E-mail: jc162@cam.ac.uk., or Valerie Dagget, Department of Medicinal Chemistry, University of Washington, Seattle, WA 98195-7610. E-mail: daggett@erebus.mchem.washington.edu.

0006-3495/01/10/2344/13 $2.00

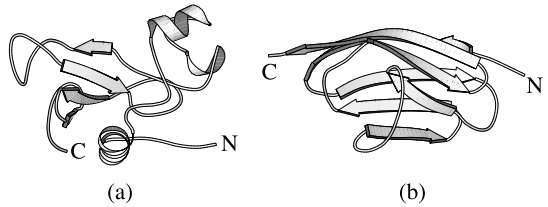

FIGURE 1 Ribbon diagrams of (*a*) barnase and (*b*) TI I27 created using MOLSCRIPT (Kraulis, 1991) from the PDB structures 1BNR (Bycroft et al., 1991) and 1TIT (Pfuhl and Pastore, 1995). The N- and C-termini are indicated to place the proteins in their AFM context.

disulfide bridges between engineered cysteines (Yang et al., 2000). However, this approach requires the knowledge of the crystal structure and has the disadvantage that the folded modules lie very close in space and are not necessarily pulled from the ends. The best solution has been achieved in the case of the I27 and I28 domains of titin by cloning multiple copies of the same gene end-to-end, to produce a polyprotein of identical modules (Carrion-Vazquez et al., 1999; Li et al., 2000). Although this approach might have been directly applied to barnase, attempts to express small barnase oligomers were not successful. We therefore used the alternative of splicing a copy of the barnase gene into an existing gene construct for TI I27, replacing every second TI I27 module (Fig. 2). This approach has the serendipitous advantage of also providing an internal standard for comparing different AFM traces.

Here we show that, although the barnase modules are folded and stable in the construct, they neither resist force to the same extent as proteins previously studied by AFM (e.g., titin and tenascin), nor do they show the regular pattern of unfolding peaks that has been seen for these other proteins. However, it is nonetheless possible to study the forces at which barnase unfolds in a meaningful way. We have also run MD simulations of forced unfolding with the inclusion of explicit solvent. These show that barnase unfolds at much lower forces than other proteins for which simulations have been run, such as titin immunoglobulin (Ig) domains (Lu et al., 1998; Lu and Schulten, 2000), fibronectin type III domains (Paci and Karplus, 1999), and elastin (B. Li, D. O. V. Alonso, B. J. Bennion, and V. Daggett, submitted for publication).

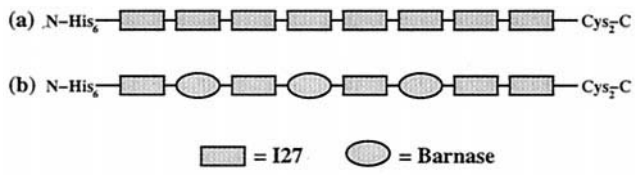

FIGURE 2 Schematic illustration of multimodular protein constructs for (*a*) a TI I27 octamer and (*b*) a barnase/I27 chimeric protein. The protein N-terminus is on the left side. The N-terminal histidine tag, His_6, used to purify the protein was left attached. At the C-terminus two cysteine residues (CC) were included to facilitate a gold-sulfur attachment to the AFM substrate.

MATERIALS AND METHODS

Cloning and protein expression

A gene construct was designed with nine distinct restriction sites, in principle allowing the cloning in of eight different domains. This was initially used to assemble a gene for eight repeats of TI I27 and will be described in more detail elsewhere. A schematic illustration of the construct is shown in Fig. 2 *a*. The C-terminus of the construct was extended by two cysteine residues to allow the protein to attach to the gold AFM substrate by gold-sulfur bonds. This gene was cloned into a modified version of the vector pRSET (Invitrogen), which adds a His_6 tag on to the N-terminus, and was transformed into C41 cells (Miroux and Walker, 1996) for expression. The construct was expressed by growing the cells to an OD_{600} of 0.4–0.7 in 2xTY media and 100 μM ampicillin and inducing with 100 μM IPTG overnight. The protein was purified from the cytosolic supernatant by affinity chromatography on a nickel-agarose column and eluted with 250 mM imidazole, leaving the His_6 tag intact to improve adhesion to the AFM tip. The purified protein was stored in phosphate-buffered saline (PBS: 10 mM phosphate buffer, 137 mM NaCl, 2.7 mM KCl), with the addition of 0.01% sodium azide to prevent bacterial and fungal growth.

A second gene with the barnase mutant H102A in the second, fourth, and sixth positions in the construct (Fig. 2 *b*) was built up by an analogous process to that for the TI I27 octamer, and expressed by the same protocol as above. The H102A mutant is inactive and can therefore be expressed intracellularly without co-expression of the inhibitor barstar, while still having similar properties to the wild type (Axe et al., 1998). In this case a flexible linker region of three Gly-Ser repeats was inserted between the barnase and TI I27 domains at each of its N- and C-termini to prevent interdomain interactions, especially important as the termini of barnase are not located at opposite ends of the protein, as is the case for TI I27 (Fig. 1).

Two three-module constructs, I27-barnase-I27 and I27-I27-I27, were also expressed to test the properties of barnase and TI I27 in the construct by solution experiments. The same procedure as above was used to express unlabeled protein. An ^{15}N-labeled sample of each protein was also produced by growth in minimal media, using $^{15}NH_4Cl$ as a the sole nitrogen source. The isolated TI I27 and the barnase mutant H102A were produced as has been described previously (Fowler and Clarke, 2001; Meiering et al., 1991).

AFM experiments

All AFM measurements were made on a molecular force probe (Asylum Research, Santa Barbara, CA), using silicon nitride cantilevers (Thermo-Microscopes, Sunnyvale, CA). The tips were calibrated in the experimental buffer, the spring constant being determined by the frequency response of the cantilever to background "white" noise (Hutter and Bechhoefer, 1993). In all cases the spring constant was within 10% of 30 pN nm^{-1}. The protein was adsorbed to the gold at sufficiently low concentration to minimize the chances of picking up two molecules (100–125 μM). A 600-μl drop of protein solution was placed on a freshly evaporated gold slide and left for 15 min, after which the excess was washed off and the bound protein covered by a fresh layer of PBS.

Force traces for both the TI I27 octamer and the I27/barnase chimeric protein were collected at a range of different pulling speeds from 100 nm s^{-1} to 5 μm s^{-1} to examine the pull-rate dependence of the force at which the protein domains unfolded. Although the microscope stage was not thermostatted, the room temperature was always in the range 20–25°C. At each pulling speed, at least 30 clear traces were recorded to get sufficient

sampling. The data were analyzed using the software Igor Pro (Wavemetrics Inc., Lake Oswego, OR).

Solution studies

Equilibrium denaturation experiments were carried out for the model three-module constructs I27-barnase-I27 and I27-I27-I27, and for the isolated barnase mutant H102A in PBS and 5 mM DTT at 25°C (protein concentration was ~1 μM in all cases). DTT was added to prevent disulfide cross-linking of unfolded protein by maintaining the cysteine residues of I27 in the reduced state. Protein was equilibrated with guanidine hydrochloride overnight and unfolding monitored by the change in fluorescence at 320 nm on excitation at 280 nm. The data were fitted to the standard two-state equilibrium curve given in Eq. 1, in which F and $[D]$ are the observed fluorescence and denaturant concentration for each data point, and the following parameters are fitted to the data: $[D]_{50\%}$, the denaturant concentration at which 50% of the protein is denatured; $m_{\text{D-N}}$, the dependence of $\Delta G_{\text{D-N}}$ on denaturant concentration; α_{N} and β_{N} are the fluorescence of the native state at 0 M denaturant and the dependence of the native state signal on denaturant, respectively; and α_{D} and β_{D} are the corresponding quantities for the denatured state (Clarke and Fersht, 1993; Fersht, 1999; Pace, 1986). R and T are the molar gas constant and temperature, as usual.

$$F = \frac{(\alpha_{\text{N}} + \beta_{\text{N}}[D]) + (\alpha_{\text{D}} + \beta_{\text{D}}[D])\exp(m_{\text{D-N}}([D] - [D]_{50\%})/RT)}{1+\exp(m_{\text{D-N}}([D] - [D]_{50\%})/RT)} \quad (1)$$

The protein stability, $\Delta G^{\text{H2O}}_{\text{D-N}}$, was calculated from the fitted values of $[D]_{50\%}$ and $m_{\text{D-N}}$ by Eq. 2.

$$\Delta G^{\text{H}_2\text{O}}_{\text{D-N}} = m_{\text{D-N}}[D]_{50\%} \quad (2)$$

Unfolding kinetics for the I27-barnase-I27 construct and isolated barnase H102A were initiated by 1:10 mixing of 11 μM protein solution with guanidine hydrochloride (GdnHCl) in PBS at 25°C. The unfolding reaction of barnase was followed using the total fluorescence above 320 nm (excitation 280 nm) in an Applied Photophysics (Leatherhead, UK) stopped-flow fluorimeter. The unfolding of the TI I27 modules in the three-module proteins was monitored after manual mixing in an Aminco Bowman fluorimeter (ThermoSpectronic, Cambridge, UK). As the unfolding rates of barnase and TI I27 are very different at the working concentration of denaturant, there is a clear separation of time scale for the unfolding kinetics of the two proteins; the initial part of the fluorescence signal may be fit to a single exponential for barnase and the remainder to an exponential for TI I27. The natural logarithm of k_{obs}, the observed unfolding rate constant, showed a linear dependence on denaturant concentration.

NMR spectroscopy

^{15}N HSQC spectra of the ^{15}N-labeled models I27-barnase-I27 and I27-I27-I27, as well as an isolated TI I27 domain, were recorded at 298 K in PBS on a Bruker (Karlsruhe, Germany) AMX-500 spectrometer.

MD simulations

To match the construct used in the AFM experiments, we added one glycine on each terminus of barnase and pulled the C_α atoms of these terminal glycines in the simulations. MD simulations were performed using an in-house version of the program ENCAD (Levitt, 1990) and a previously described force field (Levitt et al., 1995, 1997). All protein and solvent atoms were explicitly present. The crystal structure of barnase (1BNI (Buckle et al., 1993)) was used as the starting structure. It was minimized for 500 steps. The protein was then solvated by a water box extending at least 10 Å in all directions. The water density was set to the experimental value (0.997 g/ml for 25°C) (Kell, 1967). The systems were prepared for MD by minimizing the water for 2000 steps, performing MD of the water for 2000 steps, minimizing the water for 2000 steps, minimizing the protein for 2000 steps, and minimizing the protein and water system for 2000 steps. After these preparatory steps the systems were heated to 298 K. MD simulations were then run using a 2-fs time step. The nonbonded list was updated every five steps, and the nonbonded cutoff was 10 Å. Periodic boundary conditions and the minimum image convention were used to reduce edge effects.

A 0.5 (low rate) or 1.0 (high rate) Å increment per step on the selected atom pair was achieved by using a 1 kcal mol^{-1} Å^{-2} force constant, followed by 50 ps of MD simulation to equilibrate at the new distance, corresponding to rates of 0.01 and 0.02 Å ps^{-1}, respectively. The restraint force (F) was calculated given this force constant and the difference between the actual end-to-end distance (x, the distance between the C_α atoms of the terminal glycines) and the designated value (x_0) for each time step ($F = k(x_0 - x)$). To obtain a detailed force curve, the restraint force was calculated every 0.2 ps, even though the designated distance (x_0) remained the same over the 50-ps intervals. The water box was enlarged twice for both simulations by resolvating the protein to ensure that there was enough water surrounding the protein during the pulling process. Resolvation of protein was achieved by taking the structure of the protein at the time points (2 and 4 ns for the low-rate simulation and 1 and 2 ns for the high-rate simulation) when the solvent box was deemed to be too small and resolvating out to 10 Å. The preparatory steps described above were then performed on this larger system and the MD simulations were run with the designated increment of the end-to-end distance. Initially, the systems contained 4491 water molecules, which was increased to 6446 (low rate) and 6534 (high rate) by the end of the simulations. Structures were saved every 0.2 ps for analysis, yielding 30,000 structures for the low-rate simulation (6 ns) and 15,000 structures for the high-rate simulation (3 ns).

RESULTS

Barnase and TI I27 are independently folded and stable in the multimodular constructs

A recombinant fragment consisting of only the first three modules (I27-barnase-I27 from the I27/barnase hybrid and I27-I27-I27 from the TI I27 octamer) were studied in solution to confirm that the stability and unfolding rate of barnase were not affected by placing it in a construct. These were chosen as sufficiently complete to represent the environment of TI I27 and barnase within the hybrid, while still being of an accessible size for NMR. ^{15}N HSQC spectra for isolated TI I27, I27-I27-I27, and I27-barnase-I27 are shown in Fig. 3. The spectra for a single TI I27 module and the triple TI I27 overlay very well (Fig. 3, *a* and *b*), indicating that the TI I27 is folded and that all the peaks for the single module are clearly resolved for the trimer. The peaks previously assigned to folded barnase (Jones et al., 1993) were clearly visible in the spectrum of the hybrid I27-barnase-I27 protein (Fig. 3 *c*), demonstrating that it, too, is folded in the construct.

Equilibrium denaturation of the I27-barnase-I27 construct gave a double transition (Fig. 4 *a* and Table 1), which was fitted to the sum of expressions for two single protein two-state denaturation curves (Eq. 1 (Fersht, 1999)). The parameters determined from this fit and those for the cor-

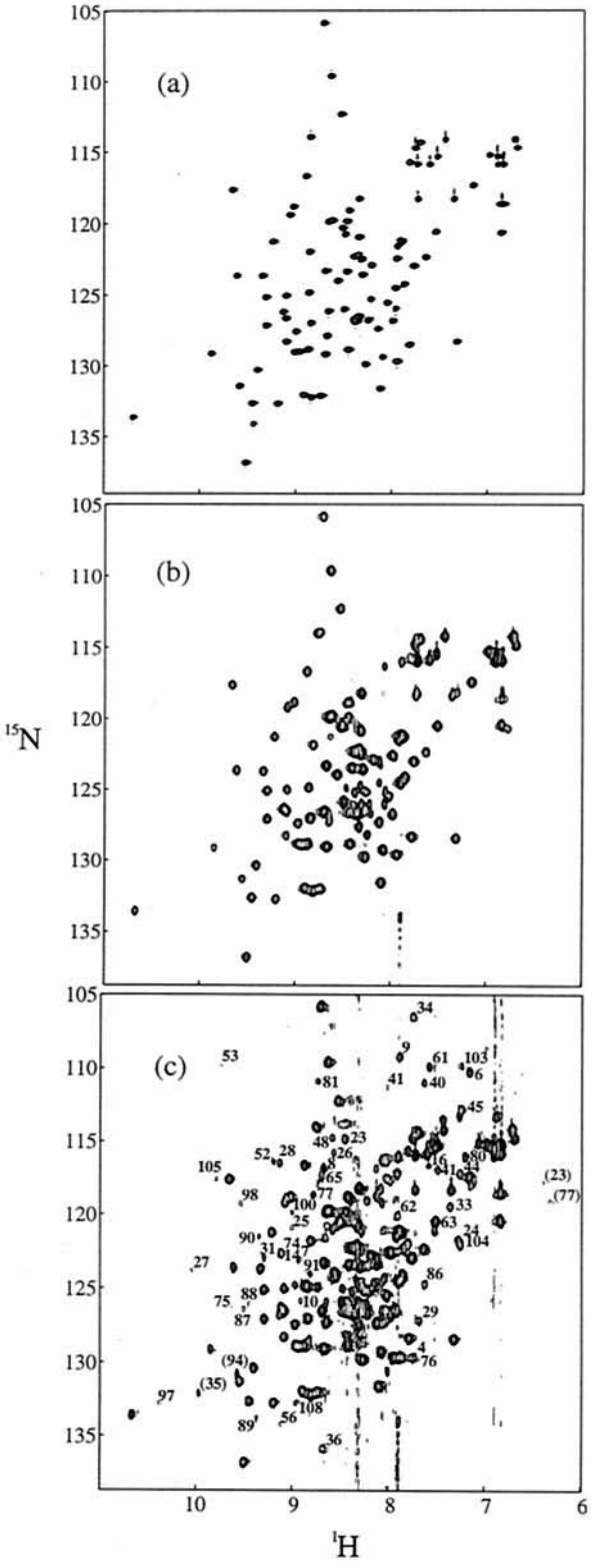

FIGURE 3 ^{1}H-^{15}N HSQC spectra of (*a*) isolated TI I27, (*b*) TI I27 trimer, (*c*) I27-barnase-I27 construct (all scales in ppm). The positions of some of the barnase backbone protons and some side chain protons (in brackets) that could be assigned based on isolated barnase chemical shift data are shown. This is a sensitive test of protein structure and indicates that each protein has the same structure when isolated and in the construct.

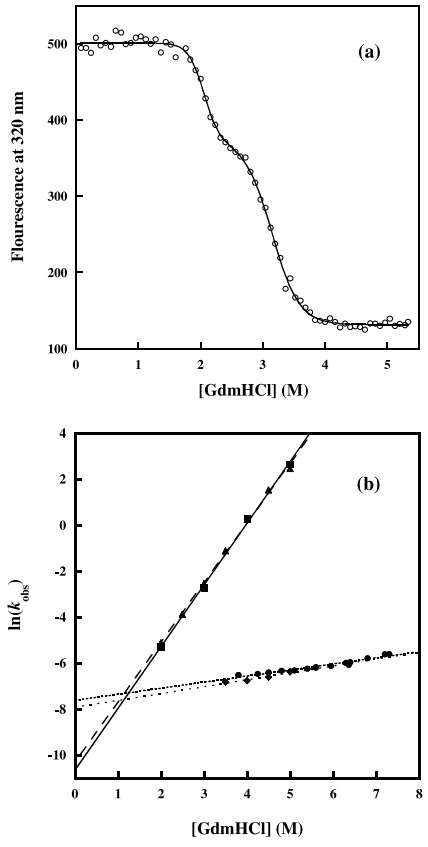

FIGURE 4 (*a*) Equilibrium denaturation curve for I27-barnase-I27 construct in guanidine hydrochloride to determine the stability of the modules in the construct. The curve was fit to the sum of two expressions for two-state denaturation, one for each protein; the contributions to the baseline were estimated from the number of tryptophan residues in each of barnase and TI I27. The transition at lower denaturant concentration corresponds to barnase. Fluorescence in arbitrary units. (*b*) Unfolding kinetics data for isolated barnase H102A (*triangles*), barnase in the I27-barnase-I27 construct (*squares*), isolated TI I27 (*circles*), and TI I27 in the above construct (*diamonds*). These show that each module has the same unfolding rate at 0 M denaturant, both in and out of the construct. The isolated TI I27 data are taken from Fowler and Clarke (2001). Units of k_{obs} are s^{-1}.

responding isolated modules are shown in Table 1. The barnase portion of the curve gives a stability of 9.8 ± 1.3 kcal mol^{-1}, which is within the error of the value determined for isolated barnase H102A (10.2 ± 0.4 kcal mol^{-1}). Thus, the protein is not only folded in the construct, it is also of comparable stability to its isolated form. The same is true of the I27 modules in this construct.

Because the force at which protein modules unfold by AFM can be related to the unfolding rate (Carrion-Vazquez et al., 1999; Rief et al., 1998a), unfolding by denaturant is the analogous bulk solution experiment. Unfolding kinetics for isolated barnase H102A and barnase in the three-module construct gave the same value, within error, for the unfolding rate constant, k_u, extrapolated to 0 M denaturant (Fig. 4 *b* and Table 2). The unfolding kinetics for isolated TI I27

TABLE 1 Parameters determined from equilibrium denaturation of barnase H102A and TI I27, both isolated and as part of a construct in PBS with 5 mM DTT at 25°C

	$m_{D\text{-}N}$ (kcal mol^{-1} M^{-1})	$[D]_{50\%}$ (M)	$\Delta G_{D\text{-}N}$ (kcal mol^{-1})
Isolated barnase	5.2 ± 0.2	1.98 ± 0.01	10.2 ± 0.4
Barnase in I27-barnase-I27 construct	4.8 ± 0.6	2.05 ± 0.02	9.8 ± 1.2
Isolated TI I27	2.5 ± 0.1	3.04 ± 0.01	7.5 ± 0.02
TI I27 in I27-barnase-I27 construct	2.7 ± 0.2	3.15 ± 0.02	8.6 ± 0.5
TI I27 in I27-I27-I27 construct	2.3 ± 0.1	3.14 ± 0.02	7.2 ± 0.3

and TI I27 in the same construct likewise extrapolate to the same unfolding rate at 0 M denaturant, so the unfolding properties of both modules are unaffected by insertion into the AFM construct.

TI I27 can be distinguished in the force traces based on its established properties

Each force-distance trace of the TI I27 octamer shows the now-characteristic sawtooth pattern, in which entropic stretching of the unfolded length of the protein causes a slow rise in force, followed by a sudden drop as each domain unfolds (an example is shown in Fig. 5 *a*). As the N-terminal end of the protein is nonspecifically attached to the tip, it may become attached at different points along the length of the polyprotein, resulting in different numbers of peaks in different pulls. Only traces in which a single protein was picked up were selected for analysis, as the interpretation of traces with multiple proteins is ambiguous: in a stretching experiment with only one protein present, the force peaks are typically of similar height with only small variations in the force of unfolding. Thus, any trace in which there is a large peak followed by a much smaller peak is likely to be due to one protein being pulled off the tip, followed by the unfolding of a domain from a second protein. In practice, there are many other tell-tale signs for the adsorption of more than one molecule to the tip, such as the presence of higher than average forces and "double" sawtooth peaks that are too close together, arising from the superposition of two traces.

The curved part of each TI I27 force peak, corresponding to the entropic elasticity of unfolded protein, was fitted to an analytical approximation to the dependence of force on extension (Eq. 3) for the inelastic worm-like chain model (Bustamante et al., 1994; Marko and Siggia, 1995), in which p is the persistence length (the correlation length of a tangent to the backbone), L is the contour length, or total length of the polymer backbone, k_B is Boltzmann's constant, T is the temperature in Kelvin, and x is the distance between the ends of the polymer.

$$F(x) = \frac{k_B T}{p}\left(\frac{1}{4(1 - x/L)^2} - \frac{1}{4} + \frac{x}{L}\right) \qquad (3)$$

A value of 3.5 Å was used for the persistence length, as this gave the best agreement with the data; it is not possible to allow p to vary freely for the fit to each force peak, as the values of the other fitted parameters then become less meaningful. The peaks for barnase could not be fitted to a pattern of worm-like chain curves with consistent increments in contour length.

The unfolding of the TI I27 octamer in Fig. 5 *a* is very similar to the previously published data using different

TABLE 2 Unfolding rate constants for barnase H102A and TI I27 as individual proteins and as part of the I27-barnase-I27 construct

	k_u (s^{-1})
Isolated barnase	$3.37 \pm 0.69 \times 10^{-5}$
Barnase in I27-barnase-I27 construct	$2.34 \pm 0.74 \times 10^{-5}$
Isolated TI I27	$4.91 \pm 0.53 \times 10^{-4}$
TI I27 in I27-barnase-I27 construct	$3.67 \pm 0.96 \times 10^{-4}$

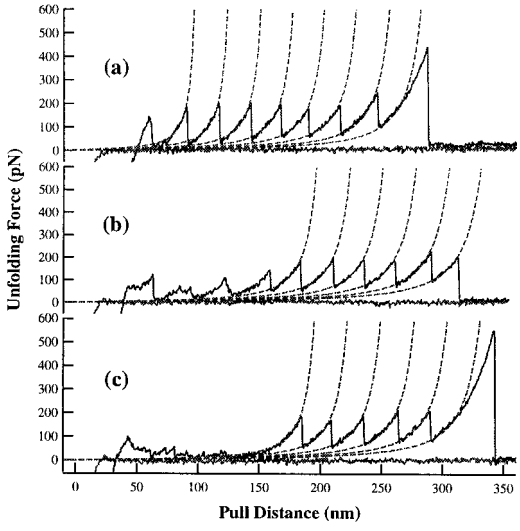

FIGURE 5 Representative AFM force-distance curves for (*a*) the TI I27 octamer, (*b* and *c*) the I27/barnase chimeric polyprotein with barnase. Both the approach and retraction force traces are shown in each case. The position of zero force has been set to the baseline without protein attached and zero displacement of the AFM head has been set to just before the protein is pulled off the surface. Worm-like chain fits to the TI I27 peaks using a persistence length of 3.5 Å are superimposed.

recombinant constructs (Carrion-Vazquez et al., 1999). Seven of the eight domains unfold in this trace and the back of each peak, corresponding to the extension of the unfolded part of the polyprotein, fits well to the worm-like chain expression in Eq. 3 with a persistence length of 3.5 Å (although the fit is better at high force (Rief et al., 1998b)), with a change in contour length between adjacent peaks of 295 ± 5 Å.

AFM experiments on the I27/barnase hybrid show different numbers of TI I27 peaks between pulls, although in many cases the full five present are observed. The peaks fit well to the same worm-like chain expression as the TI I27 octamer, with the same persistence length and change in contour length between peaks; this agreement confirms that the properties of TI I27 in the hybrid construct are unchanged from those of the octamer. TI I27 therefore provides a useful internal reference for the barnase/I27 chimeric protein.

Distinct peaks are observed for barnase in the hybrid protein

As the barnase modules were located in positions 2, 4, and 6 of the construct, the presence of at least three peaks for TI I27 guarantees that a barnase insert must lie within the segment pulled, while four and five peaks ensure that 2 and 3 barnase modules must have been pulled, respectively. The presence of barnase in the I27/barnase traces is manifested by a very heterogenous set of peaks at low force appearing before the TI I27 peaks. In some traces there are clearly a full three peaks for barnase (as in Fig. 5 *b*), although the position and height of these varies considerably, while in others, there are fewer peaks or none at all (Fig. 5 *c*).

Since we have already established that the solution properties of barnase in the multimodular construct are not altered from those of the isolated protein, we must rationalize the force-distance traces in Fig. 5 in terms of conditions unique to the AFM. It is evident that the regions of the polyprotein containing barnase have actually been pulled in both parts *b* and *c* of Fig. 5: not only are all five TI I27 peaks present, but the distance from when the tip is drawn off the surface (the small peak at ~50 nm extension) to the point at which the first TI I27 module unfolds is ~120 nm, which corresponds approximately to the length of three unfolded 110-residue barnase segments, each with an additional six Gly-Ser repeats. This conclusion is strengthened by the absence of such initial low force events from all traces of the TI I27 octamer.

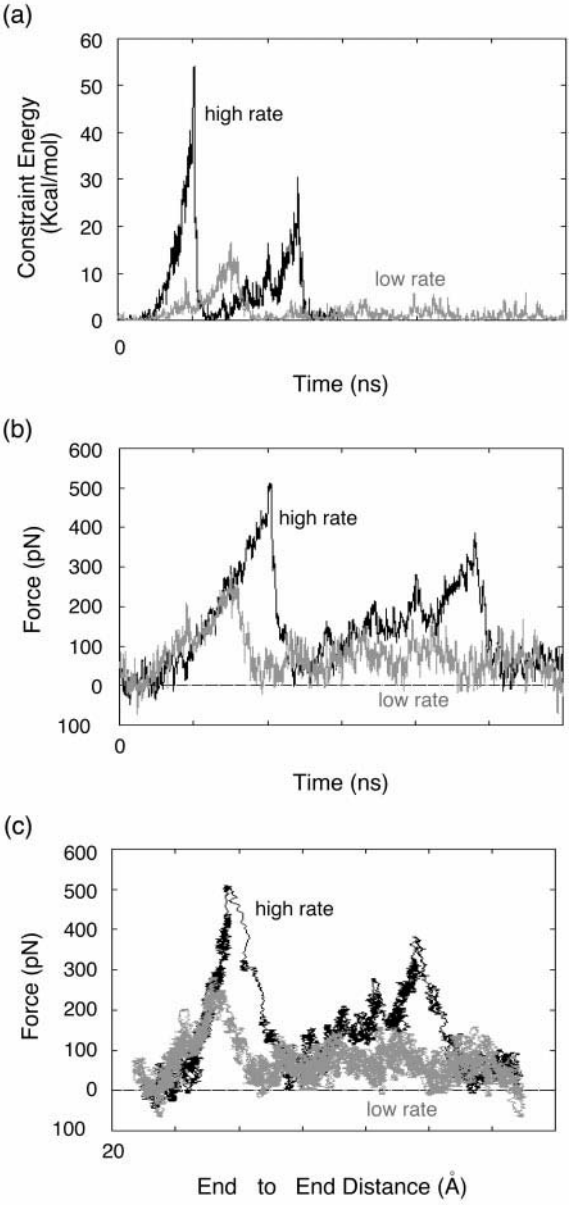

FIGURE 6 Response of barnase to pulling in the force-induced unfolding simulations: (*a*) the constraint energy as a function of time for the low- (0.01 Å ps^{-1}, *gray*) and high-rate simulations (0.02 Å ps^{-1}, *black*); (*b*) the constraint force as a function of time. The time of the high-rate simulation has been doubled, showing that the main force peaks appear at similar relative positions; (*c*) the constraint force as a function of end-to-end distance, the low-rate and high-rate simulations appear to undergo similar events as the main force peaks occur at the same extension. The extension can be obtained by subtracting 24 Å, the end-to-end distance of the starting structure.

Molecular dynamics simulations of pulling give low force peaks

In an attempt to better understand the behavior of barnase under force, two MD simulations were performed in which the protein was pulled at different speeds. The evolution of the constraint force ($F = k(x - x_0)$) as a function of time is plotted in Fig. 6 *b*. For the low-rate (0.01 Å ps^{-1} or 1×10^9 nm s^{-1}) simulation (*gray curve* in Fig. 6), the force is low at the beginning of the pulling process, but rises at 1.3 ns to a peak at 1.7 ns as the protein resists the pulling force. A

rapid drop in the constraint energy is observed after 1.7 ns as the protein passes the transition state for force-induced unfolding (Fig. 6 *a*). In addition, the maximum in the constraint force rises when the pulling speed is increased (compare *gray* and *black curves* in Fig. 6), in agreement with the experimental finding that the force at which modules unfold also increases with pulling speed. As shown in Fig. 6 *c*, the largest peaks in the constraint force are 269 pN (at 0.01 Å ps^{-1}) and 507 pN (at 0.02 Å ps^{-1}), which correspond to end-to-end distances of 35–38 Å or extensions of 11–14 Å. Structures corresponding to the major peaks are provided in Fig. 7 with contact maps showing their side- and main-chain interactions. The structural properties of the force-induced transition states are independent of pulling speed (Fig. 7). The overall unfolding of the protein is also independent of the pulling speed (Fig. 8).

Several properties of barnase, C_α root-mean-square-deviation (RMSD), radius of gyration, and solvent-accessible surface area, were monitored over time (Figures describing those data are available from the authors.). The change in these properties showed a distinct delay at the position of the force peaks (Fig. 6) in the high-rate simulation; but the properties increased smoothly in the low-rate simulation. A cluster analysis of pairwise C_α RMSDs indicated clear structural ensembles for both simulations at the positions corresponding to the force peaks (Figures describing these data are available from the authors). Moreover, the transition-state clusters for the simulations using different rates are quite similar to one another (see Fig. 7), again demonstrating that the structural properties of the transition states are independent of pulling speed in the simulations.

DISCUSSION

The distribution of barnase forced unfolding events

The properties of barnase under force do not fit the pattern of most other proteins that have been unfolded by AFM. Barnase does not show a discernible pattern of regularly spaced peaks with a fixed increment in contour length. Instead, the peaks occur at much lower forces, and sometimes only very low peaks are observed, which we could not confidently distinguish from the baseline noise (see Fig. 5, *b* and *c*). The low, irregular peaks for barnase may be caused by the different parts of the protein unfolding in separate steps, or possibly by the protein unfolding by alternative pathways under force.

Instead of attempting to analyze the barnase unfolding peaks by means of worm-like chain fitting, we have plotted histograms of the unfolding forces for the TI I27 multimer and the barnase/I27 hybrid. These contain the most important information available from the AFM data, namely the force at which the protein unfolds, which is related to its unfolding rate on the force-perturbed energy landscape. An example for data collected at a pulling speed of 300 nm s^{-1} is given in Fig. 9. The force distribution for the I27/barnase hybrid (Fig. 9 *b*) shows a large peak at ~190 pN that approximately matches the position of the peak in the TI I27 octamer force distribution (Fig. 9 *a*). There is a subsidiary peak at ~70 pN arising from the peaks attributable to barnase. The ratio of the peak heights is not the same as the ratio of TI I27 to barnase modules in the hybrid, due to the traces with no barnase peaks, and also to the caution exercised in not picking small peaks that may result from background noise or interactions between the tip and the surface or proteins on the surface. Nonetheless, the separation of unfolding events for the two proteins suggests that it is possible to study proteins such as barnase, which cannot be expressed intracellularly in soluble form, in our construct.

The dependence of unfolding force on pulling speed was analyzed for both barnase and TI I27 by dividing the bimodal force distribution into two populations along the minimum between the peaks and taking separate averages of unfolding force for peaks above and below this value. The results are shown in Fig. 10, which also gives the dependence of TI I27 unfolding force on pulling speed in the TI I27 octamer. This plot shows that the force at which TI I27 unfolds in the chimeric protein depends linearly on the logarithm of the pulling rate, in a similar fashion to that of the modules in the TI I27 multimer. The unfolding forces for TI I27 in the construct appear very slightly higher than for those in the multimer, possibly because of the exclusion of low force peaks due to our division of unfolding events before averaging. An additional factor is the slight increase in peak height with extension, even for TI I27 homopolyproteins, because of the elastic compliance of the AFM tip (Evans and Ritchie, 1999); because we only count the last five peaks of the chimeric protein, which is longer than the I27 octamer to begin with, the average unfolding force would be overestimated. Following these arguments, the reverse might be expected for barnase, but the force distribution for that protein is probably also biased toward higher forces because of the exclusion from the analysis of low force peaks that were not reliably distinguishable from background noise. Furthermore, the unfolding forces attributable to barnase follow a similar linear relationship to the logarithm of the pulling speed. A theoretical description based on Kramers' theory (Evans and Ritchie, 1999) predicts a linear relationship between unfolding force and the logarithm of the loading rate r_f, defined by $r_f = kv$, where k is the spring constant of the cantilever and v is the pulling speed. As all of our experiments used a similar spring constant (within 10% of 30 pN nm^{-1}), a linear relation is indeed predicted to hold between unfolding force and the logarithm of pulling speed. This is another piece of evidence confirming that the peaks we

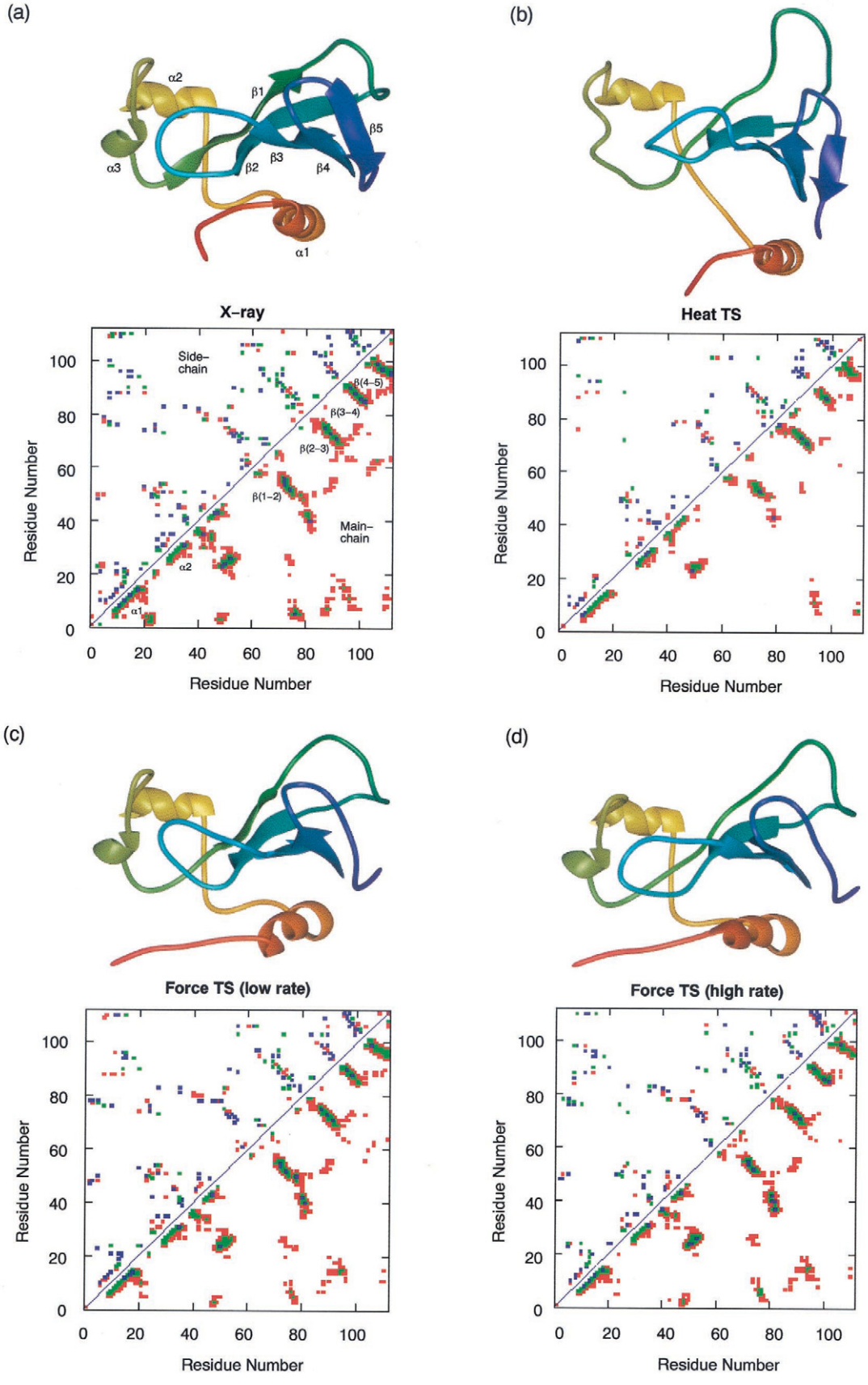
(a)
α2
β1
β5
α3
β2
β3
β4
α1
X–ray
Side–chain
β(4–5)
β(3–4)
β(2–3)
β(1–2)
Main–chain
α2
α1
Residue Number
0
20
40
60
80
100
(b)
Heat TS
Residue Number
(c)
Force TS (low rate)
Residue Number
(d)
Force TS (high rate)
Residue Number

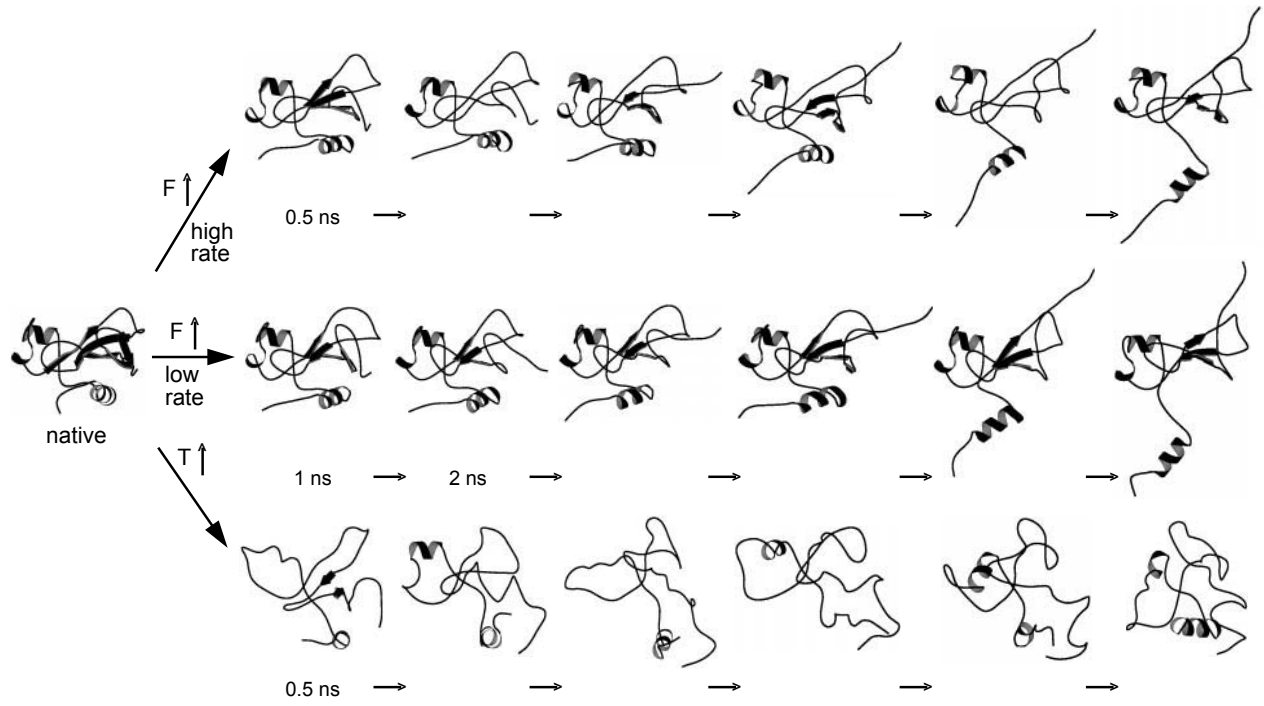

FIGURE 8 Comparison of simulated unfolding pathways under force (F) and at high temperature (T). In the force-induced unfolding simulations barnase passes the transition state by disrupting the packing interaction at the termini while the whole molecule remains compact and native-like. However, in the heat-induced unfolding simulation, the structural changes are distributed throughout the protein and barnase becomes more expanded after the transition state. Moreover, the force-induced unfolding of barnase at the high rate shows a second force peak (Fig. 6) corresponding to the further separation of α_1 from the main body of the protein (compare 2- and 2.5-ns structures of the high-rate simulation). In contrast, the intermediates from the heat-induced unfolding, represented by the 0.5-ns structure (the actual intermediate is populated from 470 to 730 ps (Li and Daggett, 1998)), show partly opened hydrophobic cores and the termini retain interactions with the protein.

have assigned to barnase in fact come from an unfolding protein.

Comparison of unfolding by force and by chemical denaturation

The above results establish that barnase and I27 behave very differently under force, despite having similar unfolding rates in bulk solution. As the two measurements are not directly comparable, a model is required to link them. The unfolding of proteins by AFM can be described as a two-state Markov process, in which the unfolding force by AFM is determined by the unfolding rate, k_u, the pulling speed, and the distance along the reaction coordinate (end-to-end length) from the folded state to the transition state, x_u (Rief et al., 1998a). In particular, the activation free energy for unfolding in the model is lowered by $F_u \cdot xu$, where F_u is the force of unfolding; this relationship is based on the assumption of a steep native energy well, so that the application of force does not cause a shift in transition state. Previous studies found that the value of k_u fitted to AFM data from this model agreed well with that determined from bulk denaturant-induced unfolding for the TI I27 (Carrion-Vazquez et al., 1999) and I28 (Li et al., 2000) domains. Although this agreement might suggest that these domains unfold by the same pathway under the two sets of conditions, it could simply be that the energy barrier to unfolding is very similar. In fact, MD simulations of forced and thermal unfolding of I27 conclude that they follow different pathways (Paci and Karplus, 2000).

If barnase and TI I27 do indeed unfold by the same pathway under force as they do in solution, and if barnase

FIGURE 7 Structures and contact maps of force- and temperature-induced unfolding transition states: (*a*) the crystal structure (native state); (*b*) the transition state for unfolding at high temperature; (*c*) the transition state for unfolding by force (low rate); and (*d*) the transition state for unfolding by force (high rate). The high-temperature TS is the average structure from 135 to 140 ps of a simulation beginning from the NMR structure (Daggett et al., 1998). The force-induced transition states are the average structures from 1.55 to 1.60 ns and 0.95 to 1.00 ns of the low- and high-rate simulations, respectively. These structures correspond to the major peaks in Fig. 6. The top left corner of the contact map shows the number of side chain interactions, N_c, with a 5.4 Å cutoff (*red*, $0 < N_c \leq 3$; *green*, $3 < N_c \leq 10$; *blue*, $N_c > 10$). The bottom right corner is the α-carbon contact map classified by atom-atom distance, d (*blue*, $d < 5$ Å; *green*, $5 < d \leq 7$ Å; *red*, $7 < d \leq 10$ Å).

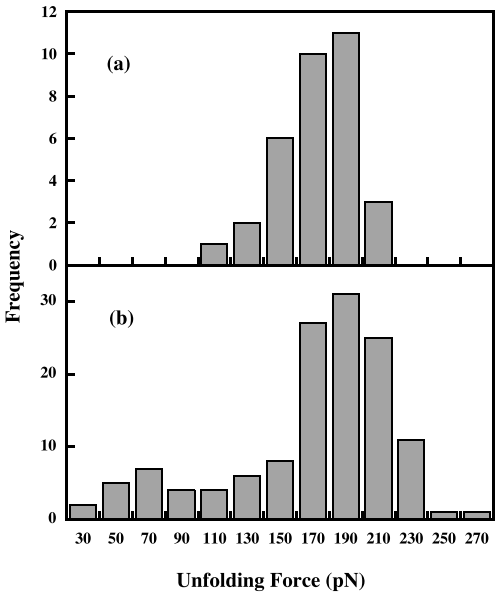

FIGURE 9 Distribution of unfolding force for (*a*) the TI I27 octamer and (*b*) the TI I27/barnase chimeric construct. In (*b*) the maximum at ~70 pN corresponds to barnase unfolding. All traces where only one protein molecule was pulled (see Results) were analyzed, and the height of all peaks that could be reliably measured (i.e., were not in the "noise") were determined and recorded.

has a similar value of x_u, then they should unfold at similar force, or possibly, barnase would unfold at a slightly higher force. [The assumption of similar x_u is justified by its theoretical relationship to the slope of the plots in Fig. 10; the slopes are very similar for barnase and I27, although they do have large associated error and x_u is known to be very sensitive to variations in slope. Because barnase has a lower value for k_u, the two-state model would predict a slightly higher unfolding force (Rief et al., 1998a).] This is clearly not the case: the solution unfolding kinetics are a poor predictor of sensitivity to force according to this two-state model. Whether each protein unfolds by the same mechanism under force and in solution cannot be determined by single pulling experiments alone, and requires either a mechanical analog of a Φ-value analysis or a detailed simulation.

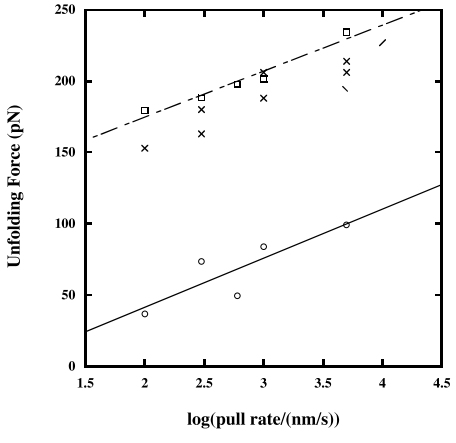

FIGURE 10 Dependence of unfolding force on the pulling speed for TI I27 in the octamer (*crosses*) and TI I27 (*squares*) and barnase (*circles*) in the hybrid protein.

MD simulations show that unfolding is initiated at the termini of barnase

During the first nanosecond of the low pulling speed (0.01 Å ps^{-1}), the protein had a very native-like structure, with a C_α RMSD of <2.0 Å from the crystal structure (Figures describing these data are available from the authors.) Both the N- and C-termini became extended as a result of the pulling process (Fig. 8). After 1.6 ns the tertiary structure became more disrupted and both termini separated from the main body of the protein. The interactions between α_2 and loop 4 also broke, and the three hydrophobic cores of barnase separated from one another. Barnase also lost ~17% of its hydrogen bonds in this process, but there was no simultaneous and cooperative breaking of hydrogen bonds, as was observed for I27 (Lu and Schulten, 2000). The high-rate simulation experienced similar effects at comparable degrees of extension. However, it has an additional force peak at ~2.5 ns (Fig. 6) corresponding to the further separation of helix 1 from the main body of the protein (Fig. 8). This second barrier may be responsible for the irregular distance between the experimental low-force barnase peaks. Overall, the simulations suggest that force acts primarily to pull the ends of the molecule from the core of the protein in a sequential manner. However, there was a peak in the force curve due to the disruption of critical packing interactions, with some pieces of secondary structure being more stable than others (Fig. 7).

Previously, we have used a conformational clustering method to identify transition states of heat-denatured proteins (Li and Daggett, 1994, 1996). When we applied this method to the low-rate trajectory, we found a cluster between 1.4 and 1.8 ns, exactly the same time period as the constraint energy peak (Figures describing these data are available from the authors.) (Fig. 6). Moreover, we can compare the two simulations with different rates using a plot of pairwise C_α RMSD over the course of the simulation. The structure differed gradually during the simulations, with a distinct block of similar structures with low RMSD to one another over the same time period as the main force peak (Figures describing these data are available from the authors). This finding suggests the existence of a strained, rigid structure just before the key structural elements (packing interactions) are broken, giving rise to a transition state on the force-induced unfolding pathway. Thus, two independent approaches, our clustering procedure and the peak in the force curves, identify the same structures as representing the major transition state. This correspon-

dence adds further support for the use of our clustering method to identify transition states in MD simulations.

Unfolding pathways at high temperature and under force are different

The force-induced transition states found in the two pulling simulations described here are much more native-like than those found by thermal denaturation simulations (Fig. 7) (Daggett et al., 1998; Li and Daggett, 1998) and by experimental studies of denaturation of barnase in solution via thermal or chemical denaturation (Serrano et al., 1992). In particular, the secondary structure is more ordered and there are more tertiary contacts in the force-derived transition state (Fig. 7). In fact, the transition states from the force-induced unfolding simulations are very native-like, far too native-like to reproduce the experimental solution Φ-values. The two force-derived transition states are very similar, however. If we continue further into each trajectory until we reach the intermediate state, the findings are similar: the intermediate state for the force-induced unfolding is highly structured in the center of the molecule, with the largest distortion localized to the ends (Fig. 8). This is not observed in the high-temperature intermediate (Li and Daggett, 1998) and the intermediate characterized experimentally using chemical denaturation (Matouschek et al., 1992), which are much more disrupted and the packing of the cores is severely compromised (see the 0.5-ns structure from the thermal denaturation simulation, Fig. 8). The ends of the molecule, particularly the C-terminus, remain in contact with the body of the protein, in contrast to the force-induced intermediate.

By comparing the order of events in the force-induced unfolding simulations with those from thermal denaturation simulations, we can address the effects that the different perturbants have on the structure. Also, we note that the simulated unfolding pathway at high temperature is in very good agreement with experiment, including the transition state, intermediates, and the denatured state (Bond et al., 1997; Daggett et al., 1998; Li and Daggett, 1998; Wong et al., 2000). Consequently, differences between the force-induced and temperature-induced unfolding pathways can tell us whether and how applied force distorts the folding process. Various snapshots from the simulations are presented in Fig. 8. When the two ends of the molecule are pulled, the transition state is reached within ~1.8 ns and corresponds to a disruption of packing interactions at the termini. This peeling away of the ends of the molecule continues over time, until just a fraction of the β-sheet exists. The α_1 helix is remarkably immune to the force; that is, it is pulled away from the protein but it retains its secondary structure. In contrast, for the early steps in the unfolding in the high-temperature simulation, structural disruptions are distributed throughout the protein and are not localized to the ends of the protein. That is not to say that barnase does not have portions of the molecule that are more ordered than others, because it does; but it does not experience the systematic unfolding from the ends of the structure seen in the forced unfolding simulations. An interesting parallel to the forced unfolding simulations was seen in previous lattice simulations of pulling (Socci et al., 2000), which were able to model the partition function of the protein under force as a collapsed globule with chain ends extending from it. Other MD simulations of stretching have shown similar structural properties in the unfolding pathway to varying extents, suggesting that this may be a general attribute of forced unfolding (Lu et al., 1998; Lu and Schulten, 2000; Paci and Karplus, 1999, 2000).

We note that although the pulling rates in the current simulations are an order of magnitude slower than previous simulations (Lu et al., 1998; Lu and Schulten, 2000), they are still six orders of magnitude faster than the experimental pulling rates. Thus, the higher unfolding forces seen in the simulations could be explained by the same reasoning as is applied to the variation of force with pulling speed in the AFM experiments: at each force the unfolding rate is the same, but at higher pulling speeds there is less time for the protein to unfold at any particular extension. Although there are small differences between the high and low pulling speed simulations, such as the second force peak at high speed (corresponding to a further separation of α_1 from the main body of barnase), the results are generally consistent: the main force peak corresponds to a very similar structure and unfolding pathway, suggesting that the mechanism for unfolding is not strongly dependent on pulling speed. In any comparison of simulation and experiment there is a possibility that at the higher pulling speeds sampled by MD a different transition state is observed than at the lower experimental pulling speeds (Evans and Ritchie, 1999). Furthermore, at the lower pulling speeds of the experiment the system has time to equilibrate. This can only be addressed when, experimentally, the structure of the transition state for unfolding is probed in molecular detail (Marszalek et al., 1999) and compared to the transition state observed in the simulations. However, the general agreement between simulation and experiment (the lower unfolding forces for barnase than observed for simulations of other proteins, and the noncooperative unfolding of barnase "in parts") encourages us to believe that the simulation can give us an insight into the experimental events.

Is mechanical strength determined by fold or function?

Both the experimental AFM results and the MD simulations show that barnase has a much lower resistance to force than TI I27, despite having a slightly slower unfolding rate in solution. How can this be interpreted in terms of the functions of the two proteins? TI I27 is under continual mechanical stress in muscle and there is evidence from immunoelectron micrograph studies that some TI I27 domains might

unfold under physiological stress (Helmes et al., 1999). Therefore, titin needs to have a sufficiently high energy barrier to unfolding to maintain native structure under stress—indeed, it is found that the unfolding rate of TI I27 is similar in bulk solution and in AFM experiments (Carrion-Vazquez et al., 1999). However, barnase does not resist force well, as it is not required for its function, and barnase is apparently unfolded by very low forces in a significant fraction of the AFM traces. This does not necessarily apply to all non-mechanical proteins: the AFM experiments on cross-linked T4 lysozyme showed regular unfolding behavior (Yang et al., 2000), with force peaks comparable to those of spectrin, a protein that is functionally required to resist force (Lenne et al., 2000; Rief et al., 1999). An important question is whether the ability to resist force is simply a property of a particular protein fold or whether it has evolved individually for function in each protein. The mechanical strength of both TI I27 (Rief et al., 1997) and fibronectin type III (fn3) domains in tenascin and titin (Rief et al., 1998b), which share a common fold, suggest the former, while the differences in their mechanical properties show that the latter is also important. In particular, differences between the fn3 domains, which have almost identical topology, highlight the role of function: fn3 domains from titin unfold at significantly higher forces than those from tenascin and fibronectin (Rief et al., 1998b).

CONCLUSIONS

We have shown that it is possible to place a globular protein, barnase, in a soluble polyprotein construct suitable for AFM. We have demonstrated that the protein is folded in the construct and has the same properties as the isolated protein in solution. By pulling a construct with a known internal reference, we were able to assess the AFM data in light of the results previously collected for the reference protein, titin I27. The distribution of unfolding peaks showed both a maximum at the correct position for TI I27 and one at significantly lower forces that must be from barnase unfolding. The force at which the barnase module unfolds has a linear dependence on the logarithm of the pulling speed, as theoretically expected for a protein unfolded by force.

Our results demonstrate that it is possible to study globular proteins such as barnase by AFM, just as has been done for structural proteins. Moreover, the construct we used should make it straightforward to clone other proteins into the same positions as barnase for study by AFM. Our method provides an alternative to the chemical linkage used for T4 lysozyme (Yang et al., 2000), which requires a known crystal structure. There is an intriguing parallel between these AFM results and experiments involving the unfolding of barnase by the mitochondrial import machinery. This process occurs by pulling on the N-terminus and has also been shown to follow a different pathway to that for solution unfolding (Huang et al., 1999).

MD simulations of unfolding by force are able to provide atomic detail regarding the mechanism of unfolding of barnase by force. Unfolding occurs primarily from the termini of the protein, with both secondary and tertiary structure being maintained for much longer in the course of unfolding than is the case for simulations of thermal unfolding. There does not appear to be a sudden loss of structure after a "key event," as was observed in simulations of the unfolding of TI I27 (Lu et al., 1998; Lu and Schulten, 2000), although there is a very native-like transition state for unfolding in which packing is disrupted.

Barnase unfolds at very much lower force than TI I27 by AFM experiment, especially when one considers that the two proteins have very similar unfolding rate constants in solution. Also, the force peaks obtained in the MD simulations are much lower for barnase than for simulations of other structural proteins using a similar protocol. It is reasonable to conclude that this is because barnase has not been selected by evolution for the purpose of withstanding force, while TI I27, tenascin, and spectrin all require this property for their function. Force spectroscopy studies on proteins that have not evolved to withstand force are consequently not expected to yield useful information about their normal function, although they are still of interest for understanding the underlying forces responsible for protein structure and folding.

We thank Alan Fersht and Julio Fernandez for providing us with the clones for barnase H102A and TI I27, respectively. We thank Darwin O. V. Alonso for help with the simulations. Robert Best is supported by a Mandela Scholarship from the Cambridge Commonwealth Trust and Jane Clarke is a Wellcome Trust Career Development Fellow.

This work was funded by the Wellcome Trust, the Medical Research Council, National Institutes of the Health Grant GM50789 (to V.D.), and Office of Naval Research Grant N00014-98-1-0477 (to V.D.).

REFERENCES

Alonso, D. O. V., S. J. DeArmond, F. E. Cohen, and V. Daggett. 2001. Mapping the early steps in the pH-induced conformational conversion of the prion protein. *Proc. Natl. Acad. Sci. U.S.A.* 98:2985–2989.

Axe, D. D., N. W. Foster, and A. R. Fersht. 1998. A search for single substitutions that eliminate enzymatic activity in a bacterial ribonuclease. *Biochemistry.* 37:7157–7166.

Bond, C. J., K.-B. Wong, J. Clarke, A. R. Fersht, and V. Daggett. 1997. Characterization of residual structure in the thermally denatured state of barnase by simulation and experiment: description of the folding pathway. *Proc. Natl. Acad. Sci. U.S.A.* 94:13409–13413.

Buckle, A. M., K. Henrick, and A. R. Fersht. 1993. Crystal structural analysis of mutations in the hydrophobic cores of barnase. *J. Mol. Biol.* 234:847–860.

Bustamante, C., J. F. Marko, E. D. Siggia, and S. Smith. 1994. Entropic elasticity of λ-phage DNA. *Science.* 265:1599–1600.

Bycroft, M., S. Ludvigsen, A. R. Fersht, and F. M. Poulsen. 1991. Determination of the three-dimensional solution structure of barnase using nuclear magnetic resonance spectroscopy. *Biochemistry.* 30:8697–8701.

Carrion-Vazquez, M., A. F. Oberhauser, S. B. Fowler, P. E. Marszalek, S. E. Broedel, J. Clarke, and J. M. Fernandez. 1999. Mechanical and chemical unfolding of a single protein: a comparison. *Proc. Natl. Acad. Sci. U.S.A.* 96:3694–3699.

Clarke, J., and A. R. Fersht. 1993. Engineered disulfide bonds as probes of the folding pathway of barnase: increasing the stability of proteins against the rate of denaturation. *Biochemistry.* 32:4322–4329.

Clausen-Schaumann, H., M. Seitz, R. Krautbauer, and H. E. Gaub. 2000. Force spectroscopy with single bio-molecules. *Curr. Opin. Struct. Biol.* 4:524–530.

Daggett, V., A. Li, and A. R. Fersht. 1998. Combined molecular dynamics and ϕ-value analysis of structure-reactivity relationships in the transition state and unfolding pathway of barnase: structural basis of Hammond and anti-Hammond effects. *J. Am. Chem. Soc.* 120:12740–12754.

Evans, E., and K. Ritchie. 1999. Strength of a weak bond connecting flexible polymer chains. *Biophys. J.* 76:2439–2447.

Fersht, A. R. 1999. Structure and Mechanism in Protein Science. W. H. Freeman and Co., New York.

Fisher, T. E., P. E. Marszalek, and J. M. Fernandez. 2000. Stretching single molecules into novel conformations using the atomic force microscope. *Nat. Struct. Biol.* 7:719–724.

Fowler, S. B., and J. Clarke. 2001. Mapping the folding pathway of an immunoglobulin domain: structural detail from phi-value analysis and movement of the transition state. *Structure.* 9:355–366.

Helmes, M., K. Trombitas, T. Centner, M. Kellermayer, S. Labeit, W. Linke, and H. Granzier. 1999. Mechanically driven contour length adjustment in rat cardiac titin's unique n2b sequence. *Circ. Res.* 84: 1339–1352.

Huang, S. H., K. S. Ratliff, M. P. Schwartz, J. M. Spenner, and A. Matouschek. 1999. Mitochondria unfold precursor proteins by unraveling them from their N-termini. *Nat. Struct. Biol.* 6:1132–1138.

Hutter, J. L., and J. Bechhoefer. 1993. Calibration of atomic-force microscope tips. *Rev. Sci. Instrum.* 64:1868–1873.

Izrailev, S., A. R. Crofts, E. A. Berry, and K. Schulten. 1999. Steered molecular dynamics simulation of the Rieske subunit motion in the cytochrome bc(1) complex. *Biophys. J.* 77:1753–1768.

Janshoff, A., M. Neitzert, Y. Oberdörfer, and H. Fuchs. 2000. Force spectroscopy of molecular systems: single molecule spectroscopy of polymers and biomolecules. *Angew. Chem. Int. Ed.* 39:3212–3237.

Jones, D. N. M., M. Bycroft, and M. J. Lubienski. 1993. Identification of the barstar binding site of barnase by NMR spectroscopy and hydrogen-deuterium exchange. *FEBS Lett.* 331:165–172.

Kell, G. S. 1967. Precise representation of volume properties of water at one atmosphere. *J. Chem. Eng. Data.* 12:66–69.

Klimov, D. K., and D. Thirumalai. 2000. Native topology determines force-induced unfolding pathways in globular proteins. *Proc. Natl. Acad. Sci. U.S.A.* 97:7254–7259.

Kraulis, P. J. 1991. MOLSCRIPT: a program to produce both detailed and schematic plots of protein structures. *J. Appl. Crystallogr.* 24:946–950.

Lenne, P.-F., A. J. Raae, S. M. Altmann, M. Saraste, and J. K. H. Hörber. 2000. States and transitions during forced unfolding of a single spectrin repeat. *FEBS Lett.* 476:124–128.

Levitt, M. 1990. ENCAD, Computer Program, Energy Calculations and Dynamics. Yeda, Rehovat, Israel.

Levitt, M., M. Hirshberg, R. Sharon, and V. Daggett. 1995. Potential-energy function and parameters for simulations of the molecular-dynamics of proteins and nucleic acids in solution. *Comp. Phys. Commun.* 91:215–231.

Levitt, M., M. Hirshberg, R. Sharon, K. E. Laidig, and V. Daggett. 1997. Calibration and testing of a water model for simulation of the molecular dynamics of proteins and nucleic acids in solution. *J. Phys. Chem. B.* 101:5051–5061.

Li, A., and V. Daggett. 1994. Characterization of the transition state of protein unfolding by use of molecular dynamics: chymotrypsin inhibitor 2. *Proc. Natl. Acad. Sci. U.S.A.* 91:10430–10434.

Li, A., and V. Daggett. 1996. Identification and characterization of the unfolding transition state of chymotrypsin inhibitor 2 by molecular dynamics simulations. *J. Mol. Biol.* 257:412–429.

Li, A., and V. Daggett. 1998. Molecular dynamics simulation of the unfolding of barnase: characterization of the major intermediate. *J. Mol. Biol.* 275:677–694.

Li, H., A. F. Oberhauser, S. B. Fowler, J. Clarke, and J. M. Fernandez. 2000. Atomic force microscopy reveals the mechanical design of a modular protein. *Proc. Natl. Acad. Sci. U.S.A.* 97:6527–6531.

Lu, H., B. Isralewitz, A. Krammer, V. Vogel, and K. Schulten. 1998. Unfolding of titin immunoglobulin domains by steered molecular dynamics simulation. *Biophys. J.* 75:662–671.

Lu, H., and K. Schulten. 2000. The key event in force-induced unfolding of titin's immunoglobulin domains. *Biophys. J.* 79:51–65.

Marko, J. F., and E. D. Siggia. 1995. Stretching DNA. *Macromolecules.* 28:8759–8770.

Marszalek, P. E., H. Lu, H. B. Li, M. Carrion-Vazquez, A. F. Oberhauser, K. Schulten, and J. M. Fernandez. 1999. Mechanical unfolding intermediates in titin modules. *Nature.* 402:100–103.

Matouschek, A., L. Serrano, and A. R. Fersht. 1992. The folding of an enzyme. 4. Structure of an intermediate in the refolding of barnase analyzed by a protein engineering procedure. *J. Mol. Biol.* 224: 819–835.

Meiering, E. M., M. Bycroft, and A. R. Fersht. 1991. Characterization of phosphate binding in the active-site of barnase by site-directed mutagenesis and NMR. *Biochemistry.* 30:11348–11356.

Miroux, B., and J. E. Walker. 1996. Over-production of proteins in *Escherichia coli*: mutant hosts that allow synthesis of some membrane proteins and globular proteins at high levels. *J. Mol. Biol.* 260:289–298.

Oberhauser, A. F., P. E. Marszalek, H. P. Erickson, and J. M. Fernandez. 1998. The molecular elasticity of the extracellular matrix protein tenascin. *Biophys. J.* 393:181–185.

Pace, C. N. 1986. Determination and analysis of urea and guanidinium denaturation curves. *Methods Enzymol.* 131:266–279.

Paci, E., and M. Karplus. 1999. Forced unfolding of fibronectin type 3 modules: an analysis by biased molecular dynamics simulations. *J. Mol. Biol.* 288:441–459.

Paci, E., and M. Karplus. 2000. Unfolding proteins by external forces and temperature: the importance of topology and energetics. *Proc. Natl. Acad. Sci. U.S.A.* 97:6521–6526.

Pfuhl, M., and A. Pastore. 1995. Tertiary structure of an immunoglobulin-like domain from the giant muscle protein titin: a new member of the I-set. *Structure.* 4:391–401.

Rief, M., J. M. Fernandez, and H. E. Gaub. 1998a. Elastically coupled two-level systems as a model for biopolymer extensibility. *Phys. Rev. Lett.* 81:4764–4767.

Rief, M., M. Gautel, F. Oesterhelt, J. M. Fernandez, and H. E. Gaub. 1997. Reversible unfolding of individual titin immunoglobulin domains by AFM. *Science.* 276:1109–1112.

Rief, M., M. Gautel, A. Schemmel, and H. E. Gaub. 1998b. The mechanical stability of immunoglobulin and fibronectin III domains in the muscle protein titin measured by atomic force microscopy. *Biophys. J.* 75:3008–3014.

Rief, M., J. Pascual, M. Saraste, and H. E. Gaub. 1999. Single molecule force spectroscopy of spectrin repeats: low unfolding forces in helix bundles. *J. Mol. Biol.* 286:553–561.

Serrano, L., A. Matouschek, and A. R. Fersht. 1992. The folding of an enzyme. 3. Structure of the transition-state for unfolding of barnase analyzed by a protein engineering procedure. *J. Mol. Biol.* 224:805–818.

Socci, N. D., J. N. Onuchic, and P. G. Wolynes. 2000. Stretching lattice models of protein folding. *Proc. Natl. Acad. Sci. U.S.A.* 96:2031–2035.

Wong, K. B., J. Clarke, J. Bond, J. L. Neira, S. M. Freund, A. R. Fersht, and V. Daggett. 2000. Towards a complete description of the structural and dynamic properties of the denatured state of barnase and the role of residual structure in folding. *J. Mol. Biol.* 296:1257–1282.

Yang, G., C. Cecconi, W. A. Baase, I. R. Vetter, W. A. Breyer, J. A. Haack, B. W. Matthews, F. W. Dahlquist, and C. Bustamante. 2000. Solid-state synthesis and mechanical unfolding of polymers of T4 lysozyme. *Proc. Natl. Acad. Sci. U.S.A.* 97:139–144.

Zhang, B., G. Xu, and J. S. Evans. 1999. A kinetic molecular model of the reversible unfolding and refolding of titin under force extension. *Biophys. J.* 77:1306–1315.